On the origin of sonoluminescence and sonochemistry

K.S. Suslick, S.J. Doktycz and E.B. Flint

School of Chemical Sciences, University of Illinois, 505 South Mathews Ave, Urbana, IL 61801, USA

Recent experimental results on the origins of sonoluminescence and sonochemistry are reviewed and the conclusion reached that most observed effects originate from thermal processes associated with a localized hot-spot created by acoustic cavitation. Sonoluminescence is definitively due to chemiluminescence from species produced thermally during cavitational collapse and is not attributable to electric microdischarge. Homogeneous sonochemistry follows the behaviour expected for high temperature thermal reactions. Ultrasonic irradiation of liquids containing solid powders dramatically increases their chemical reactivity and improves chemical yields for a wide range of synthetically useful heterogeneous reactions. Shock waves generated from the cavitational hot-spot cause high velocity interparticle collisions in such slurries. Brittle solids are shock fragmented, which increases surface area. This increase in reactive surface provides for substantial increases in chemical reactivity. For malleable metal powders, these collisions are sufficiently violent to remove surface oxide coatings and to induce local melting at the site of impact for most metals.

Keywords: acoustic cavitation; sonochemistry; sonoluminescence; ultrasonic cleaning; powders; slurries

Acoustic cavitation

Sonochemistry does not arise from a direct interaction of sound with molecular species. The acoustic wavelengths of ultrasound (15 kHz to 10 MHz) in typical liquids range from 10 to 0.01 cm, which are much greater than molecular dimensions. No direct coupling of the acoustic field with chemical species is responsible for its chemical effects. Sonochemistry derives primarily from acoustic cavitation[1].

Cavitation[2] has at least three discrete stages: nucleation, bubble growth, and, under proper conditions, implosive collapse. The dynamics of cavity growth and collapse are strikingly dependent on the local environment. Cavity collapse in a homogeneous liquid is very different from cavitation near an extended liquid solid interface.

Formation of cavities in liquids is a nucleated process. The theoretical tensile strength of a pure liquid is so large as to preclude cavity formation simply from the negative pressure of an acoustic expansion wave under typical laboratory conditions. Instead, nucleation of bubbles occurs at weak points in the liquid, such as gas-filled crevices in suspended particulate matter or from transient microbubbles from prior cavitation events[3].

The growth of a bubble in an acoustic field has been an area of much theoretical work. This area has been extensively reviewed[2,4]. The mechanisms of bubble growth have been developed from mathematical descriptions of bubble motion. The limited experimental work has guided and supported the theoretical descriptions.

At moderate acoustic intensities, a small gas bubble in a liquid can be long lived and may undergo many oscillations, driven by the sound field. A bubble will oscillate around a mean radius if three processes have near equal rates: the rate of growth of the bubble during rarefaction, the rate of contraction during compression, and the rate of change of the sound field from rarefaction to compression. The intrinsic properties of the liquid (i.e. viscosity, density and surface tension) determine the rates of expansion and compression of the bubble in the liquid. This oscillation of bubble size in a weak to moderate acoustic field is known as stable cavitation.

Such a resonating bubble in an acoustic field can grow by a process called rectified diffusion. Growth by this process occurs because the rate of diffusion of gas in and out of a bubble is dependent on the surface area of the bubble. Thus, more gas diffuses into the bubble during rarefaction, when the bubble is large, than diffuses out of the bubble during compression, when it is small. Bubbles can grow substantially by this process over many acoustic cycles. Rectified diffusion is most commonly observed in gassy (near saturated) liquids.

Presented at the Sonochemistry Symposium of the International Congress of Pacific Basin Societies: Pacifichem 89, Honolulu, HI, USA, 22 December 1989

0041-624X/90/050280-11

At high acoustic intensities, another mechanism for bubble growth becomes important. The conditions necessary for stable cavitation (nearly equal rates of expansion, compression and change in pressure) are met only for small bubbles. At high acoustic intensities, the inertia of a large bubble prevents it from responding rapidly enough to the sound field to maintain resonance. The momentum of the bubble from one rarefaction phase can cause the bubble to expand until the next rarefaction phase, which further accelerates the bubble's growth.

Once the cavity has overgrown, it can no longer efficiently absorb energy from the sound field and can no longer sustain itself. The forces that cause the bubble to contract, such as the surface tension and the static pressure, start to dominate. At this point the bubble is very unstable. The surrounding liquid rushes in and the cavity implodes.

Homogeneous sonochemistry and sonoluminescence

There have been two general classes of explanations for the origins of homogeneous sonochemistry and sonoluminescence: thermal and electrical. The dominant paradigm is currently a thermal theory. Compression of a gas generates heat. The rapid compression of gas and vapour during cavitational collapse leads to nearly adiabatic heating of the contents of the bubble, simply because thermal transport is slower than the collapse. Thus a short lived, localized hot-spot is formed in an otherwise cold liquid. Homogeneous sonochemistry and sonoluminescence arise from hot molecules and radicals formed in the cavitational hot-spot by bond cleavage or rearrangement, followed by atomic and radical recombination, and thermal and chemical quenching[5,6]. This theory best accounts for the large current body of data, and the majority of workers in the area interpret their data in terms of the thermal theory. Some of the most important data used to support the thermal theory will be discussed.

Electrical theories of sonoluminescence and sonochemistry were among the first to be developed, but they have generally fallen into disfavour in recent times. Margulis, after discrediting prior electrical theories[7], has recently developed another one[8,9]. In this review we will also discuss the salient points of this new electrical theory and it's inconsistency with experiment.

Evidence for the thermal theory

The thermal theory of sonochemistry holds that the chemical effects of ultrasound in homogeneous systems come from the rapid heating of the contents of cavitational bubbles. The chemistry that this heating produces is dominated by homolytic bond cleavage, which produces high energy atomic and radical species. Sonoluminescence is produced by the recombination of these radicals into small molecules, which emit because they are formed in the excited state, or because they are heated to temperatures where excited states are thermally populated. Evidence for this theory comes from a wide variety of sources, and it is the only theory that accounts for all observations.

Hydrodynamic theory

The theoretical development of the hot-spot theory of sonochemistry preceded experimental verification. The majority of the work in this area has focused on the equations of bubble motion in an acoustic field. Several authors have used these equations and derived others to calculate the temperatures reached upon cavitation[10–16]. Calculated values for the maximum temperature reached during implosive bubble collapse along with the gas in the cavitational bubble, are presented in *Table 1*. These studies all start with the adiabatic collapse of a gas filled bubble, and then apply various corrections for parameters that affect the maximum temperature, such as thermal conductivity of the gas, condensation of the vapour, reactions of the gas, and radial distribution of the temperature inside the bubble, etc. These calculations are difficult to compare for a number of reasons. Most importantly, the relative importance of the various corrections is difficult to establish. Furthermore in these studies, the assumptions of initial conditions vary widely, which has a significant impact on the calculations. Nonetheless, these models do suggest that very high temperatures can be reached upon cavitational collapse.

Experimental evidence

The thermal theory of sonochemistry and sonoluminescence proposes that high temperatures formed in the cavitation event are the source of the observed sonochemistry, and that the majority of this chemistry is of a radical or atomic nature. The experimental evidence for the high temperatures reached during cavitation come from studies of both sonoluminescence and sonochemistry. The thermal theory is consistent with studies on the effect of dissolved gas and vapour pressure on sonochemical rates and sonoluminescence intensities; with the timing of the sonoluminescence flash; and with the nature of the observed chemical reactivity. The radical and atomic nature of sonochemical reactions have been deduced from studies of sonoluminescence spectra, product analyses, and detection or trapping of intermediates.

Table 1 Theoretical temperature of the cavitation event: calculations from mathematical hydrodynamic models

Authors	Year	Dissolved gas	Maximum temperature (K)	Ref.
Noltink and Neppiras	1951	N_2	9500	9
Hickling	1963	N_2	3500	10
Fogler	1969	CO_2	1900	11
Young	1976	Ar	1650	12
Fujikawa and Akamatsu	1980	Air	6700	13
Margulis and Dmitrieva	1982	Air	5300	14

Table 2 Theoretical temperatures after adiabatic compression

Gas	$\gamma = C_p/C_v$	Theoretical temperatures (K) Compression ratios, V_i/V_f [r_i/r_f] 2 [1.26]	4 [1.59]	10 [2.15]
He	1.67	945	3007	13892
Ar	1.67	945	3007	13892
H_2	1.41	789	2097	7634
O_2	1.40	784	2068	7460
N_2	1.40	784	2068	7460
NH_3	1.31	736	1826	6064
CO_2	1.30	731	1801	5926
C_2H_6	1.20	682	1568	4707

For an ideal gas, the temperature, pressure, and volume of a system that has been adiabatically compressed change according to Equation (1), where γ is the ratio of the thermal conductivities, $\gamma = C_p/C_v$.

$$P_i/P_f = T_i/T_f = (V_f/V_i)^{\gamma} \quad (1)$$

The final temperature calculated for bubbles filled with various gases initially a 297 K adiabatically compressed by various amounts are given in *Table 2*. These calculations indicate that significant temperatures can be achieved by modest compression ratios, and that γ has a significant effect on the final temperature that is reached. Experimentally, increasing γ of the dissolved gas in sonochemical reactions increases reaction rates as predicted by the thermal theory. For example, the rate of hydrolysis of CCl_4 is strongly dependent on the γ of the dissolved gas[16].

If γ is the only significant parameter of the dissolved gas that determines the temperature of the cavitation event, then sonochemical rates and sonoluminescence intensities should be the same under the noble gases, since all $\gamma = 1.67$. This is *not* the observed behaviour, however. Sonochemical and sonoluminescent processes also show a strong dependence on the thermal conductivity of the dissolved gas[13,17,18]. These results indicate that bubble collapse is not completely adiabatic, and that the thermal conductivity of the gas in the bubble affects the rate of heat transferred to the surroundings during compression.

A bubble contains not only the gas that is dissolved in the liquid, but also vapour from the liquid itself. The amount of vapour in the bubble depends on the vapour pressure of the liquid, which is strongly dependent on the temperature of the bulk liquid. The effect of changing vapour pressure on various sonochemical and sonoluminescence processes has been examined[19-22]. These studies show a striking difference between sonochemistry and all other chemistry: the rate of homogeneous sonochemical reactions decrease as the bulk temperature is increased. As the ambient temperature increases, the solvent vapour pressure increases, which decreases the efficacy of cavitational collapse.

The vapour pressure of the liquid is thought to affect the temperature of the cavitation event in three ways. First, liquid vapour will, in general, decrease the γ of the contents of the bubble, since polyatomic molecules have $\gamma < 1.2$. Secondly, vapour in the bubble decreases the maximum temperature of the cavitation event because the vapour is compressible[14]. Condensation of vapour to liquid requires energy, which is therefore unavailable for heating. Thirdly, sonochemical bond cleavage is an endothermic process that also decreases the maximum temperature of the cavitation event[12].

The observed effect of the liquid vapour pressure on sonoluminescence intensity is a strong confirmation of the thermal theory. In virtually all homogeneous sonochemical reactions, the rate of the reaction is highly dependent on the vapour pressure of the solvent system. In most systems, the reaction coefficient (k_{obs}) can be related to the system vapour pressure (V_p) as in Equation (2).

$$\log k_{obs} = -mV_p/T_0 + n \quad (2)$$

where m is a positive constant that contains the activation energy of the reaction, ambient pressure and γ, and n is relatable to the activation entropy of the reaction. This experimentally derived expression is as expected for heating of the cativational bubble with nearly adiabatic collapse[20-22].

The timing of the sonoluminescence flash in relation to the phase of the sound field can be used as a test of the thermal theory of sonoluminescence. From the discussion of acoustic cavitation presented above, sonoluminescence is expected only during the compression phase of the sound field. In their review of sonoluminescence, Reynolds and Walton[23] cite more than ten measurements of the timing of sonoluminescence with regard to the phase of the sound field. There are gross inconsistencies among these various studies, with some authors concluding that sonoluminescence occurred during the compression phase, some stating that it happened during the expansion phase, and some saying it happened during both phases!

The first definitive work in this area is from Jarman and Taylor[24]. A toroidal transducer with a well characterized sound field was used for this study. This experiment demonstrates that sonoluminescence occurs during the compression phase of the sound cycle, which is consistent with the thermal theory. Jarman and Taylor were of the opinion that the disagreements between the various measurements of this phenomenon were due both to poor characterization of the sound fields used to generate the sonoluminescence, and to artifactual phase shifts in the electrical and optical signals caused by the electronics. Other recent experiments, where care was taken to set up and characterize a standing wave sound field with phase adjusted electronics have verified that sonoluminescence occurs, as expected, only during the compression cycle of the sound field (L.A. Crum, personal communication).

When low-resolution sonoluminescence spectra of water under a variety of dissolved gases were first reported, the broad emission was fitted with black-body emission curves[25], as proposed in the Neppiras-Noltink theory of sonoluminescence[10]. Higher resolution sonoluminescence spectra, however, showed emission bands from molecular species in the u.v. region of the spectrum. The sonoluminescence spectrum[26] from water under Ar showed a well defined emission peak from OH at 306 nm. The continuum in the visible region of the spectrum was conclusively shown to be from molecular species because different regions of the spectrum could be selectively quenched by the addition of nitric acid[27]. It was proposed that radical and atomic reactions caused by the high temperature of the cavitation event were the source of the excited state molecules.

Our recent data on the sonoluminescence of hydrocarbons[28,29] are only consistent with the hot-spot

chemiluminescence model of sonoluminescence[30]. This emission is clearly *not* blackbody radiation, since it shows vibronically resolved bands that can be definitively assigned to emission from excited state diatomic molecules, as shown in *Figures 1* and *2*. The sonoluminescence spectra change dramatically upon the addition of small amounts of reactive gas, e.g. O_2, N_2, and NH_3, which would not be expected to change the temperature significantly. The emitting species observed (excited states of C_2, CN, OH, CO_2, etc.) are those also observed in flame spectroscopy[31].

Thus, the sonoluminescence of hydrocarbon liquids is consistent with the hot-spot chemiluminescence model of sonoluminescence i.e. that radicals and atoms formed by bond dissociation are the intermediates responsible for emission. All of the emitting species that are conclusively identified by their band spectra (C_2, CN, CH, OH) are formed in other high temperature processes[31], as are the species with broader spectra that have been proposed (C_2H, CO_2, Cl_2). The change in the sonoluminescence intensity from alkanes as a function of vapour pressure is consistent with the expected temperature dependence of the cavitational hot-spot. The sonoluminescence intensity as a function of diatomic gas concentration is also consistent with the hot-spot model[29].

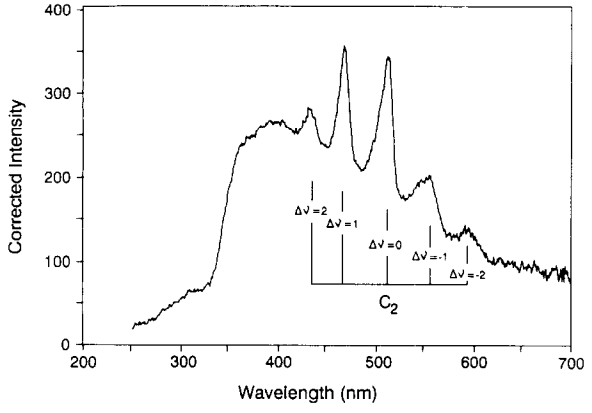

Figure 1 Sonoluminescence spectrum of dodecane[29] under Ar at 4°C

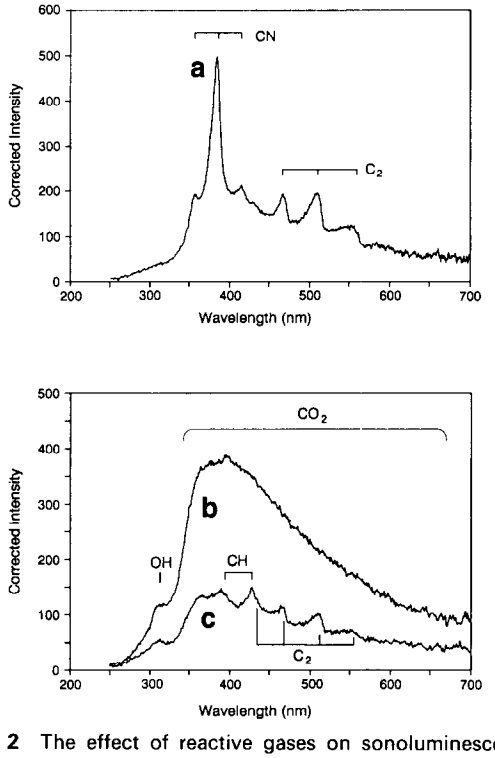

Figure 2 The effect of reactive gases on sonoluminescence[29]. Peaks from excited state emission of C_2, CN, CO_2, OH, and CH, are indicated. Curve a, sonoluminescence spectrum from dodecane under 15% N_2/85% Ar at 4°C; curve b, sonoluminescence spectrum from dodecane under O_2 at 4°C; curve c, sonoluminescence spectrum from dodecane under 10% O_2/90% Ar, 4°C

Further evidence for the intermediacy of radicals in sonochemical reactions is found in spin trapping experiments. Electron paramagnetic resonance spin-trapping is a technique where short-lived radicals are converted into long-lived radicals, which are then detected. Hydrogen atoms and hydroxyl radicals have been detected with this method after ultrasonic irradiation of both aqueous and non-aqueous solutions[34].

The analysis of the products of various homogeneous sonochemical reactions are also consistent with the hot-spot mechanism. Ultrasonic irradiation of water in the presence of a mixture of $^{14}N-^{14}N$ and $^{15}N-^{15}N$ leads to the production of scrambled $^{14}N-^{15}N$, consistent with a high temperature process[35]. It was proposed that radical and atomic fragments of water, namely H· and OH·, attacked the nitrogen molecules and caused them to dissociate. As another example, the ultrasonic degradation products of decane were analysed[19]. The primary products were H_2, C_2H_4, and C_2H_2, with smaller amounts of C_3 through C_9 l-alkenes and alkanes. The product distribution in this study was similar to the distribution found for the high temperature pyrolysis of decane. The Rice radical chain mechanism, which was originally demonstrated for alkane pyrolysis, was consistent with the products of alkane sonolysis.

Cavitational temperature

Because of the transient nature of the cavitation event, measurement of the conditions generated during bubble collapse by conventional methods is not possible. Chemical reactions themselves, however, can be used to probe reaction conditions. The effective temperature of cavitational collapse can be determined by the use of competing unimolecular reactions whose rate dependencies on temperature have already been measured. Tsang[37] developed this 'comparative-rate chemical thermometry' for gas-phase shock-tube studies, and Suslick *et al.* extended its use to determine the effective temperature reached during cavitational collapse[38,39]. The sonochemical ligand substitutions of volatile metal carbonyls were used as the comparative rate probes.

Hammerton in our labs first discovered that there were in fact two sonochemical reaction sites[40]. The liquid phase concentration of the dissolved metal carbonyl can be changed independently from its gas phase concentration (its vapour pressure) by changing the ambient temperature. The rates of these reactions were monitored as a function of these separable concentrations, showing that one reaction site occurred in the bubble's gas phase and that the second took place in a phase that was initially a liquid. The latter presumably corresponds to a shell of liquid around the bubble heated after collapse.

In these kinetic studies, the relative sonochemical rates in both the gas phase and initially liquid phase reaction sites were determined. In combination with the known temperature behaviour of these reactions, the conditions present during cavitational collapse in both reaction zones could then be measured. The effective temperature

of these hot spots is in excess of 5000 K in the gas phase reaction zone and ≈ 2000 K in the initially liquid zone[38,39]. Of course, the comparative rate data represent only a composite temperature: during the cavitational collapse, the temperature has a highly dynamic profile, as well as a spatial temperature gradient in the liquid surrounding the gas phase hot spot. A more realistic view of the temporal and spatial evolution of the liquid zone temperature may be obtained with a heat transport model calculated by an explicit method of finite differencing[38]. This simple model includes only conductive heat transport and has no adjustable parameters; nonetheless, it agrees reasonably well with the data. The model also gives us a sense of scale concerning the liquid reaction zone. It extends only ≈ 200 nm from the bubble surface and has an effective lifetime of less than 2 μs after collapse. The size of the heated shell corresponds to a reactive liquid layer about 500 molecules thick.

Very recently we have completed an alternative measurement of the cavitational temperature based on the vibronically resolved sonoluminescent emission of excited state C_2 from ultrasonic irradiation of hydrocarbon solvents[41]. This more direct probe of the temperature is in excellent agreement with the comparative rate thermometry determination.

Electrical theories of sonoluminescence

Electrical theories of sonoluminescence have also been proposed. These theories assert that charging of gas-filled bubbles in solution occurs, producing an electrical microdischarge that is the source of light. The mechanism for formation of a sizeable charge separation, which is the primary requirement for a microdischarge, must be explained by all the electrical theories of sonoluminescence or sonochemistry. The original electrical proposal[42] argued that if the bubble were shaped like a lens the two sides of the bubble would be close enough to discharge. However, no mechanism was proposed for the creation of the charge separation. Another proposal[43] was that charges initially on the surface of a bubble were concentrated upon collapse, and that discharge occurred between the gas and the charged interface. Yet another theory proposed that anions accumulated on the surface of the bubbles due to the neutralization of cations by free electrons[44].

Margulis[8,9] has very recently developed a microdischarge theory using these concepts and new ones to propose a mechanism for charge separation. This theory starts with a bubble at larger than resonant size that has been made from the coalescence of smaller bubbles. This type of bubble, called a large deformed bubble, has been seen and photographed when the frequency of the sound used is in the 10 to 200 Hz range. A process observed with such a bubble is the formation of a smaller bubble off the side of the large one. Margulis has proposed that this bubble formation is the source of the charge separation. As the smaller bubble is pinched off, the charges from a large area of the large bubble are assumed, to concentrate onto a small area of the small bubble. The rate of formation of the bubble is assumed to be faster than the rate of diffusion of charges along its surface, so a large negative charge is proposed to accumulate on the smaller bubble where it separates from the large bubble. A discharge is then proposed to occur through the small bubble to equalize the charges.

Two experimental studies have been cited as support for this electrical model. The first was a measurement of the timing of the sonoluminescence flash[45], which reported that sonoluminescence occurred at a point of negative pressure in the sound field. The study by Margulis on the timing of the sonoluminescence flash contains no mention of the parameters Jarman and Taylor[24] cite as being important in this type of work: very careful characterization of the sound field and good control of the phase shift behaviour of the electronics. Due to the difficulty of these experiments, errors in determining the timing of the sonoluminescence flash have not been unusual.

The second was a study of the temporal behaviour of the flash[46], which reported that it had a very steep rise time (< 2 ns) and a longer fall time, on the order of 10–15 ns. Similar temporal behaviour was seen from an actual microdischarge, and the similarity of these two curves was cited as evidence for the electrical theory. While there is an apparent similarity between the temporal behaviour of sonoluminescence and the microdischarge, there is no reason to believe that it is indicative of a similar mechanism. Margulis[8,9] asserts that the rise time for sonoluminescence from a hot-spot should be in the 100 ns range. Other studies, both theoretical and experimental, indicate that a 2 ns rise time is consistent with cavitational collapse in a 20 kHz sound field[2,3]. Margulis also states that if the sonoluminescence is thermal in origin, the temporal behavior of the pulse should be symmetrical in time since the equations from simple hydrodynamic models for cavitational temperature are symmetric about the minimum radius. This assumption, however, is clearly incorrect: there is an inherent asymmetry in sonochemical or sonoluminescent events. The formation of the high energy species responsible for sonochemistry and sonoluminescence cannot occur until the temperature of the cavitation event reaches a certain level, but after their formation, they can continue to emit or react, even as the temperature drops.

Another significant drawback of the electrical theory of sonoluminescence is its inability to explain sonoluminescence from non-aqueous, non-polar liquids such as alkanes. The electrical theory would predict that because there is no charging of the bubbles, there should be no sonoluminescence. This is clearly not the case: sonoluminescence from organic liquids can be orders of magnitude more intense than that from water[28,29]. Similarly, Margulis' own observations of sonoluminescence from liquid metals dismisses charge separation as a viable theory.

Finally, the sonoluminescence spectra of hydrocarbons in the presence of N_2 are not consistent with electrical discharge theories[8,9]. While emission from C_2 and CN is observed from both electrical discharges and from flames, emission from excited state N_2 and N_2^+ is seen only with electrical discharges[32]. In our sonoluminescence spectra, only emission from C_2 and CN excited states is present; there is no emission from N_2 or N_2^+. As another example, electrical discharge through Cl_2 results in emission[33] from excited-state Cl_2^+. Again, sonoluminescence spectra fail to show any such emission. The emission spectra of N_2, N_2^+, and Cl_2^+ are all easily identifiable banded spectra. Their absence in sonoluminescence spectra highlight the deficiency of electrical discharge theories.

Heterogeneous sonochemistry

Cavitation near extended solid surfaces

Cavitational collapse near extended liquid–solid interfaces differs greatly from cavitation in pure liquids. The perturbation of the sound field near the interface induces an asymmetric collapse of cavitating bubbles. This deformation is self-reinforcing, and it sends a fast-moving stream of liquid through the cavity at the surface with velocities about 100 m/s. This microjet impact has been observed in high-speed microcinemagraphic sequences[47] and by flash microphotography[48]. Such impacts leave behind characteristic microscopic pitting in the surface. Cavitation induced surface damage of extended surfaces can also occur from shock waves created by cavity collapse in the liquid.

The impingement of microjets and shock waves on the surface causes the localized erosion responsible for ultrasonic cleaning and many of the sonochemical effects on heterogeneous reactions. The cavitational erosion of metals generates newly exposed, highly heated surfaces and ejects metal (in unknown form, perhaps as atoms or small clusters) from the surface. The importance of this process to corrosion and erosion phenomena of metals and machinery has been thoroughly reviewed elsewhere[49].

Bubble collapse will be distorted by a solid surface only if the surface is several times larger than the resonance bubble size[2,4]. Thus, for solid particles smaller than ≈ 200 μm, jet formation cannot occur with ultrasonic frequencies of ≈ 20 kHz. In these cases, however, the shock waves created by homogeneous cavitation can create high velocity interparticle collisions. As discussed later, we have discovered that the turbulent flow and shockwaves produced by intense ultrasound can drive metal particles together at sufficiently high speeds to induce effective melting at the point of collision[50].

Synthetic applications

The use of high intensity ultrasound to enhance the reactivity of metals as stoichiometric reagents has become a routine synthetic technique for many heterogeneous organic and organometallic reactions[1,5,51–55]. This is especially true for the reactive metals, e.g., Mg, Li or Zn. The effects are quite general and apply to reactive inorganic salts and to main group reagents as well. The synthetic use of ultrasound in such systems originated with the early work of Renaud and the more recent studies of Luche[52], Boudjouk[55], Mason[53], and others, as well as our own. Rate enhancements of more than tenfold are common, yields are often substantially improved, and by-products avoided.

Despite the synthetic utility of ultrasound to chemical synthesis, the mechanism of rate enhancements in both stoichiometric and catalytic reactions of metals remained largely unexplored. To probe the origins of heterogeneous sonochemistry and sonocatalysis we utilized a threefold approach: monitor the effect of ultrasonic irradiation on the kinetics of the chemical reactivity of the solids; examine the effects of irradiation on surface morphology and size distributions of powders and solids; and determine the surface composition by surface microanalytical depth profiles. This approach has proved effective in a series of studies of the sonochemistry of transition metal powders[50,56–60].

Ultrasonic irradiation of liquids containing metal powders leads to dramatic changes in morphology. After sonication of such slurries, we observed smoothing of individual particles and agglomeration of particles into extended aggregates (*Figure 3*). The surface composition of these powders was determined by Auger electron spectroscopy and sputtered neutral mass spectrometry. Such elemental depth profiles revealed that ultrasonic irradiation effectively removed the surface oxide coating from Zn, Ni, and Cu powders (*Figure 4*). The removal of such passivating coatings dramatically improves rates for a variety of both stoichiometric and catalytic reactions.

For example, Casadonte[57] discovered in our laboratory that hydrogenation of alkenes by Ni powder is enormously enhanced ($>10^5$-fold) by ultrasonic irradiation[55]. The interesting effects of ultrasonic irradiation on the surface morphology include smoothing of the initially crystalline surface and agglomeration of small particles. Both effects are attributable to inter-particle collisons caused by cavitational shock waves. Auger electron spectroscopy reveals that there is a striking decrease in the thickness of the oxide coat after ultrasonic irradiation, just as in the case of stoichiometric reactions of Cu and Zn. The removal of this passivating layer explains the $>10^5$-fold increase observed in catalytic activity.

Another application of sonochemistry to difficult heterogeneous systems was discovered in collaboration with Green and his students at Oxford University: the process of molecular intercalation[61,62]. The adsorption of organic or inorganic compounds as guest molecules between the atomic sheets of layered inorganic solid hosts permits the systematic change of optical, electronic, and catalytic properties. Important technological applications of these materials include lithium batteries, hydrodesulphurization catalysts, and solid lubricants. The kinetics of intercalation, however, are generally extremely slow, and syntheses usually require high temperatures and very long reaction times. High-intensity ultrasound dramatically increases the rates of intercalation (by as much as 200-fold) of a wide range of compounds (including amines, metallocenes, and metal sulphur clusters) into various layered inorganic solids (such as ZrS_2, V_2O_5, TaS_2, MoS_2, and MoO_3). Scanning electron microscopy of the layered solids coupled to chemical kinetics studies demonstrated that the origin of the observed rate enhancements comes from particle fragmentation (which dramatically increases surface areas), and to a lesser extent from surface damage. The ability of high intensity ultrasound to rapidly form uniform dispersions of micrometer-sized powders of brittle materials had not been previously recognized. The activation of brittle, non-metallic heterogeneous reagents often arises from this effect. As discussed below, such fragmentation comes from interparticle collisions driven by cavitational shock waves.

Effects of interparticle collisions

Most solid–liquid heterogeneous reactions are carried out with powdered solids. As discussed earlier, however, microjet impact cannot occur during cavitation of liquids with fine powders. In the presence of small particles, normal cavitational collapse will still occur, and shock waves will propagate from the hot-spot so produced.

Such shock waves can cause small particles to collide into one another with great force, producing interparticle

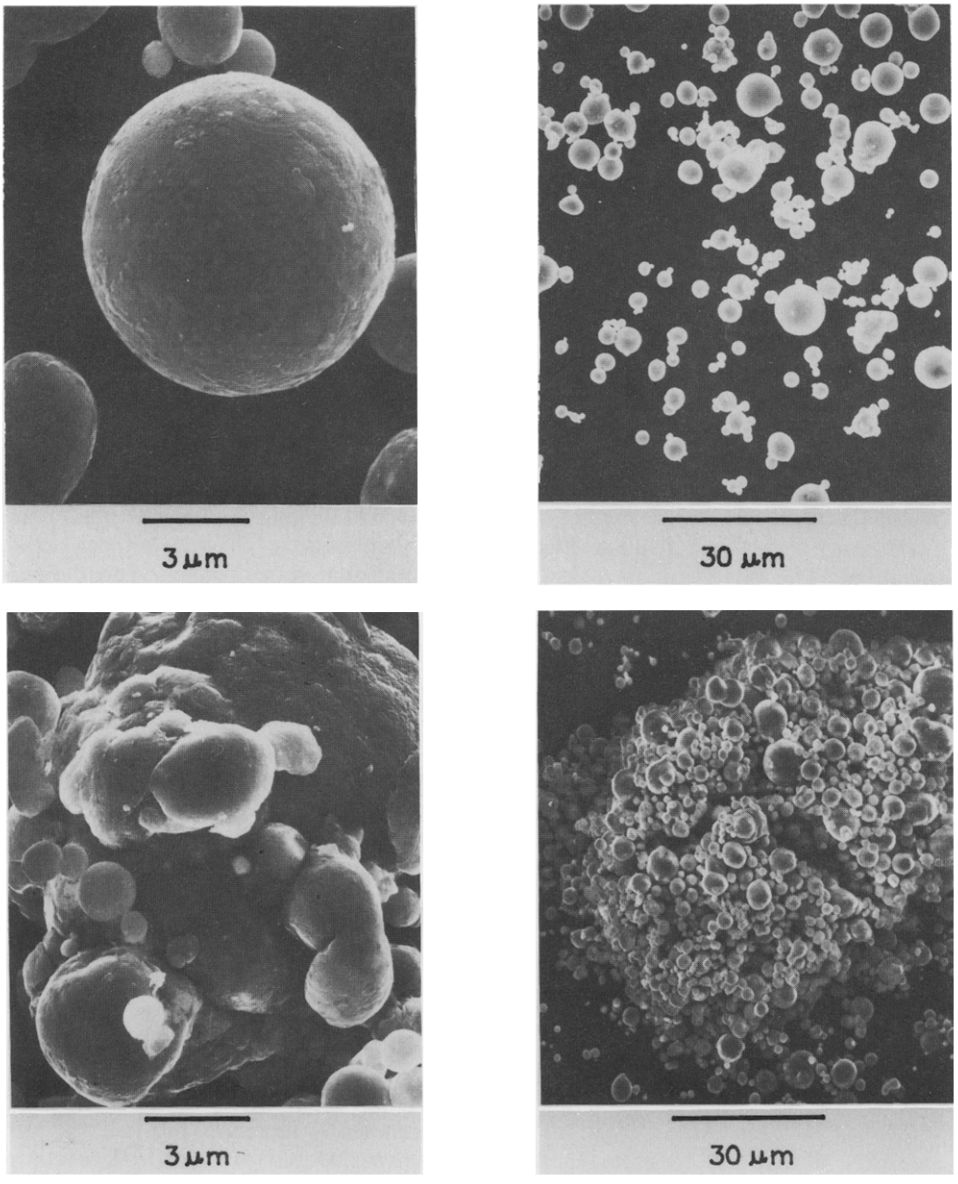

Figure 3 Scanning electron micrographs of Zn powder before (upper) and after 30 min (lower) ultrasonic irradiation; obtained on a Hitachi S-800 SEM

melting, as illustrated in the scanning electron micrograph (SEM) shown in *Figure 5* for Zn powder. The two Zn particles, originally separate spheres, are fused together after impact. The formation of a neck of Zn metal joining the two particles can be seen. We believe that this neck originates from the rapid cooling of the effectively molten collision zone as the colliding particles rebound immediately after impact. Further evidence of the heating that occurs at the neck region is indicated by the polymerization of reactive liquids, such as dioxane (*Figure 5*), that occurs only at the site of interparticle impact.

Irradiation of slurries containing two different metal powders result in similar fusings. As in the case of the Zn, a melted neck joins the two particles. Scanning Auger electron spectroscopy elemental dot maps show that the melted neck area is comprised mainly of the lower melting point metal, as shown in *Figure 6* for Fe and Sn.

In order to probe the maximum temperatures reached during interparticle collisions, we irradiated a series of transition metal powders as slurries in decane[50]. Scanning electron micrographs were obtained before and after irradiation. The effects of ultrasonic irradiation on particle agglomeration and surface morphology are given in *Table 3*. SEMs for ≈ 10 μm average diameter powders of chromium (m.p. 1857°C), molybdenum (m.p. 2617°C), and tungsten (m.p. 3410°C) are shown in *Figure 7*. Before irradiation the Cr powder consists of non-aggregated crystalline particles. After 30 min irradiation, extensive interparticle fusion occurs, which results in the formation of large agglomerates. In addition, the original crystallinity of the individual particles has been reduced by irradiation and the surface of the agglomerates shows considerable smoothing. Mo (which melts at 2617°C) also shows agglomeration and interparticle melting after 30 min irradiation, but other effects of the interparticle collisions have diminished. For Mo, neck formation is reduced to spot-welds and no change in surface morphology occurs, even with extended irradiation of 4 h.

In striking contrast to other metal powders, ultrasonic irradiation of tungsten (W) powder produces no appreciable effects, as shown in *Figure 7*. No appreciable agglomeration and no changes in surface morphology of the W are noted, even with 4h irradiation. W melts at 3419°C. We therefore conclude that the peak effective temperatures reached during interparticle collisions must fall between roughly

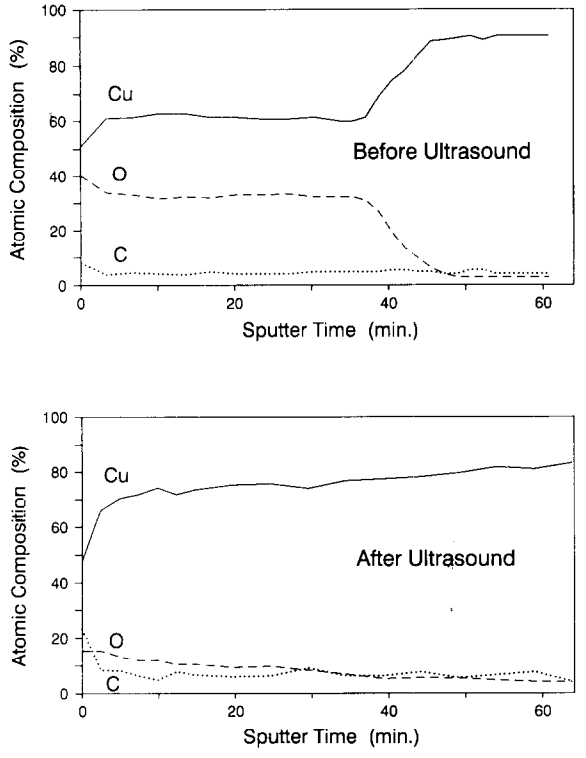

Figure 4 Surface composition depth profiles of 75 μm Cu powder. Depth profiles were derived from Auger electron spectra obtained on a Physical Electronics 595 Multiprobe spectrometer with Xe^+ sputtering at 3 KeV. Sputtering times correspond to an erosion rate of $\approx$ 270 Å/min. The upper depth profile is of a Cu sample before ultrasonic irradiation. The lower depth profile is of a Cu sample after 4 h ultrasonic irradiation in dimethylformamide at 288 K

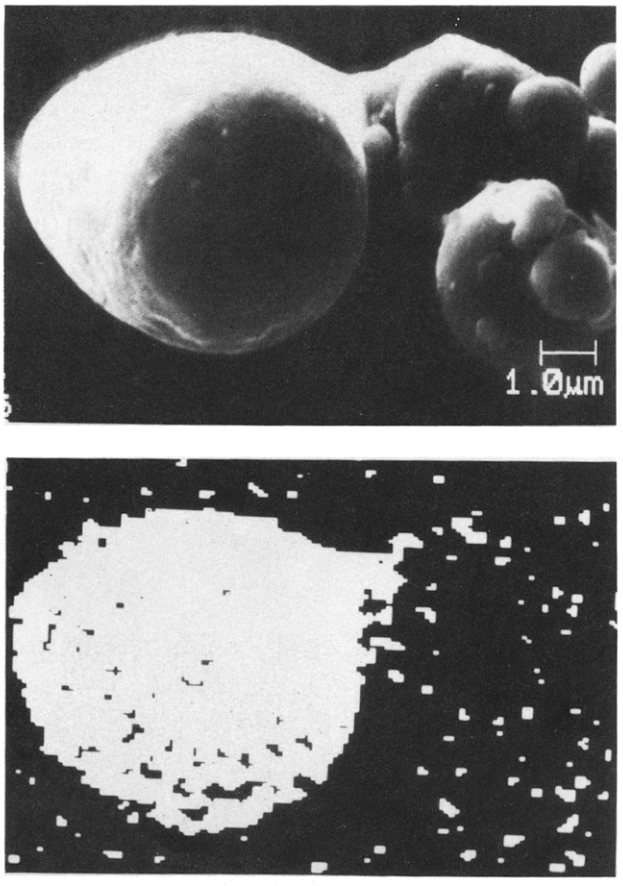

Figure 6 Upper, scanning electron micrograph of an interparticle collision induced by ultrasound between Sn and Fe particles. Lower, elemental Sn dot map showing the Sn particle and melted neck region[60]. Determined by scanning Auger electron spectroscopy on a Perkin-Elmer 660 spectrometer at 20 kV and 0.46 nA current

2600°C and 3400°C, for particles of $\approx$ 10 μm diameter.

Interparticle velocities will depend on various experimental parameters, including particle size, liquid viscosity, solid fraction in the slurry, ambient gas, and vapour pressure, among others. Sufficiently large particles will be only minimally accelerated by the cavitation shock waves. Interparticle collisions still occur and surface morphology and chemical reactivity can be affected, but particle agglomeration will not occur[60] for example, as with 160 μm diameter Ni. In sufficiently viscous liquids, the velocity of interparticle collisions will probably be diminished. We have observed, however, similar interparticle collision in various synthetically useful liquids, including several alkanes (n-octane through n-tetradecane), dimethylformade, and dioxane. Further work is in progress.

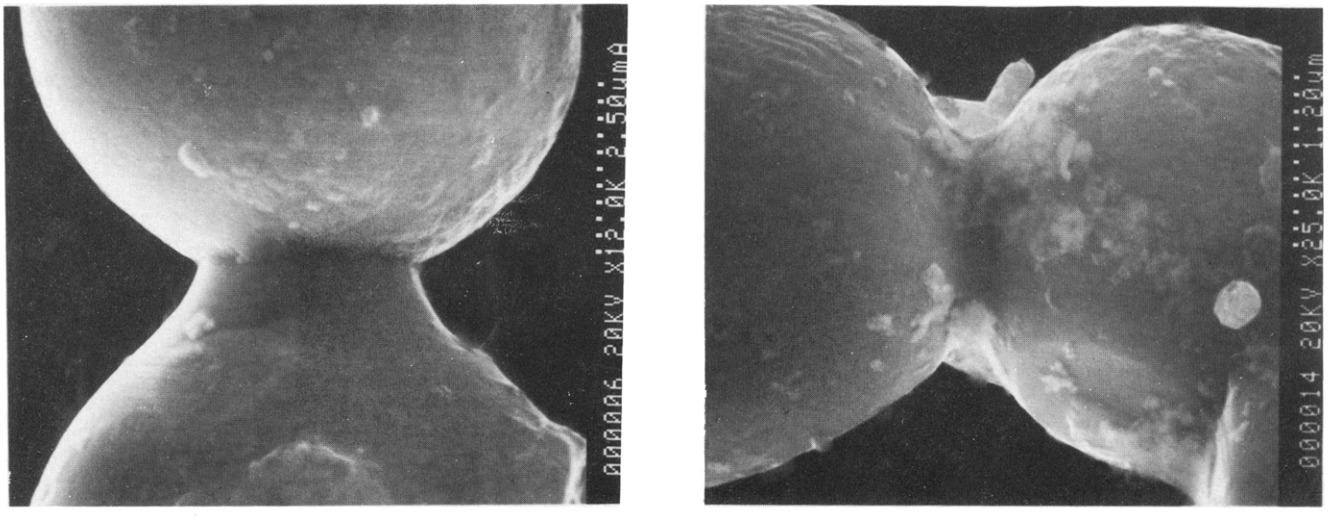

Figure 5 Scanning electron micrograph of 5 μm average diameter Zn powder after ultrasonic irradiation. Neck formation from localized melting is caused by high velocity collisions. The metal powders were irradiated 30 min at 15°C in freshly distilled decane (left) or dioxane (right) under Ar at 20 kHz and 50 W/cm^2. Note the polymerization of dioxane only in the immediate vicinity of the melted neck. Scanning electron micrographs were taken on a Hitachi S-800 at 20 kV accelerating voltage

Table 3 Effects of ultrasound on metal powders. Metal powders with ≈ 10 μm diameters were suspended in decane at 15°C and ultrasonically irradiated for 30 min at 50 W/cm^2 and 20 kHz

Metal	Melting point (°C)	Extent of agglomeration	Degree of surface smoothing
Sn	232	+ +	+ +
Zn	420	+ +	+ +
Cu	1083	+ +	+ +
Ni	1453	+ +	+ +
Fe	1535	+ +	+ +
Cr	1857	+ +	+ +
Mo	2617	+	–
W	3410	– –	– –

We can also estimate the velocity and time of interparticle impact from these studies. If we assme that full melting of the neck region of merged particles occurred during collision, then the energy of the collision can be calculated from heat capacities and heats of fusion applied to the volumes of the interparticle necks determined by SEM. Because the collisions have a range of interparticle velocities, there is an observed range of neck sizes in each experiment. Typically, the interparticle neck volumes are between 0.5 and 6 μm^3. The calculated energy to melt the neck represents a lower bound of the kinetic energy of impact and thus a lower bound estimate of the impact velocity. Repeating this calculation for Zn–Zn, Cr–Cr, and Fe–Sn interparticle collisions from many micrographs

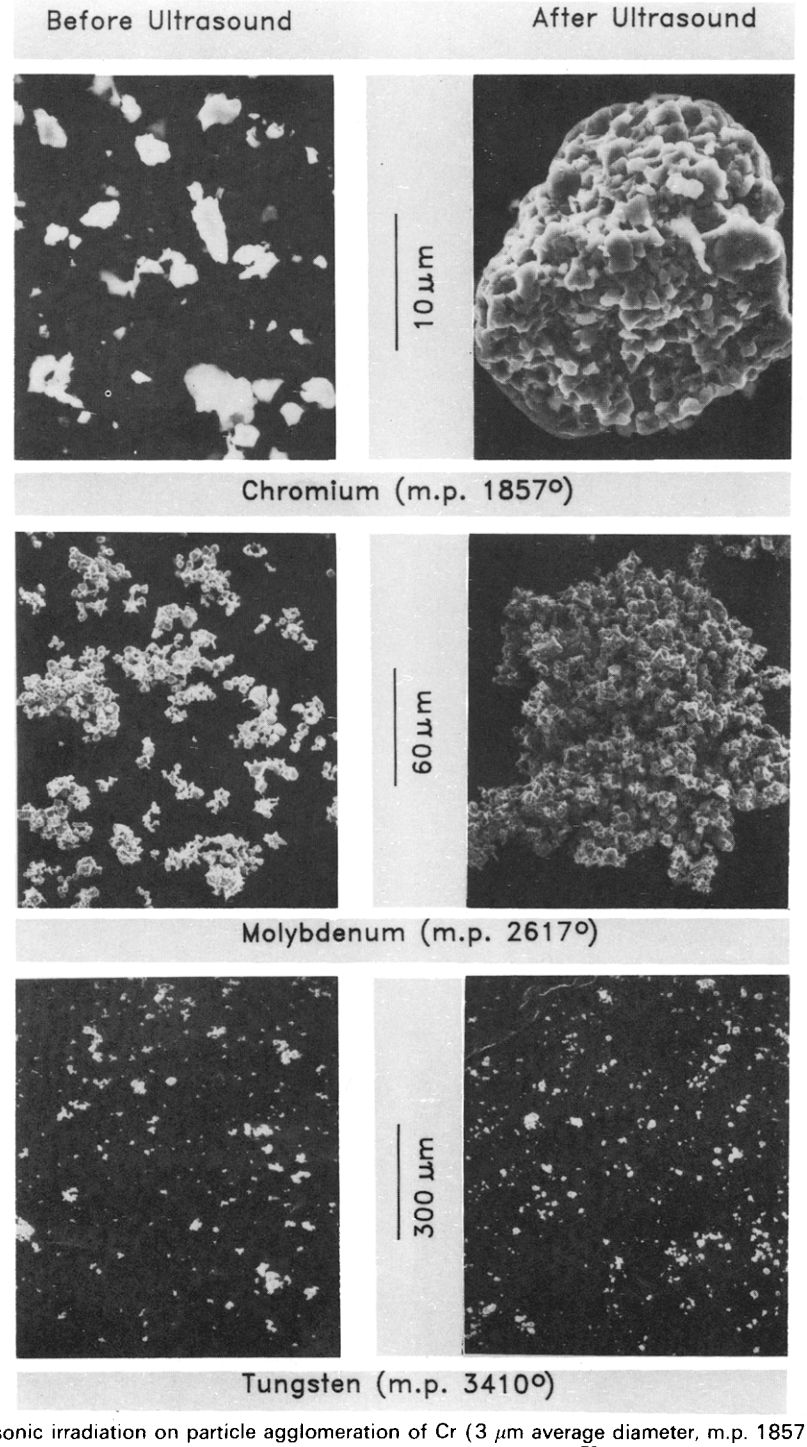

Figure 7 The effect of ultrasonic irradiation on particle agglomeration of Cr (3 μm average diameter, m.p. 1857°C), Mo (10 μm average diameter, m.p. 2617°C), and W (10 μm average diameter, m.p. 3410°C) in decane slurries[50]. The metal powders were irradiated for 30 min in decane slurries of 2.5% metal v/v

results in estimates of impact velocities ranging from 100 to 500 m s^{-1}, for particles of ≈ 10 μm diameter.

Shock waves in a liquid must have velocities greater than the speed of sound (in hydrocarbons, roughly 1100 m s^{-1}). From thermodynamic models of underwater bomb blasts, velocities of infinitesimal particles can be calculated from the shock wave pressure[63]. Laser-induced cavitation in water produces[64] shock wave pressures as large as 300 MPa. Infinitesimal particle velocities of 160 m s^{-1} are calculated from shock waves of this size, in excellent agreement with our experimental observations on 10 μm diameter powders.

Finally, we can estimate roughly the time of cooling of the melted neck formed during impact. If the colliding particles recoil with a velocity on the order of 500 m s^{-1} (an upper bound), then a neck with length of 0.5 μm would be formed in roughly a nanosecond. This is a reasonable lower limit estimate of the cooling time following collision of 10 μm diameter powders. The extreme, but short-lived, conditions created during these interparticle collisions will also have a high pressure component; some plastic deformation below a true melting of the collision zone may also occur.

The synthetic utility of ultrasound on heterogeneous liquid solid chemical reactions has been very well established over the past few years. We have now quantified the high energy conditions created during ultrasonic irradiation of powders in liquids. The importance of high velocity interparticle collisions during ultrasonic irradiation of slurries is established. Metal particles which collide head-on do so with enough energy to cause localized melting at the site of impact. This reveals hot, reactive metal surfaces and contributes to the chemical effects of ultrasound. For powders of brittle, refractory materials (such as layered inorganic solids), such collisions induce particle fragmentation with substantial increases in surface area and thus reactivity.

Conclusions

Most of the chemical effects ultrasound originate from thermal processes associated with a localized hot-spot created by acoustic cavitation. Sonoluminescence is definitively due to chemiluminescence from species produced thermally during cavitational collapse and is *not* attributable to electric microdischarge. Homogeneous sonochemistry and sonoluminescence follow the behaviour expected for high temperature thermal reactions.

Ultrasonic irradiation of solid–liquid systems has proved useful for a variety of heterogeneous sonochemical reactions. Shock waves generated from the cavitational hot-spot cause high velocity interparticle collisions in such slurries. Brittle solids are shock fragmented, which increases surface area. This increase in reactive surface provides for substantial increases in chemical reactivity. For malleable metal powders, these collisions are sufficiently violent to remove surface oxide coatings and to induce local melting at the site of impact for most metals. This provides for highly reactive surfaces and improves chemical yields and rates for a variety of synthetically useful reactions.

Acknowledgements

The help of Professor Alexander Scheeline and Dr Dominick J. Casadonte is greatly appreciated. Thanks are also duc Dr Irena Dulmer, Dr Christopher Loxton, and Nancy Finnegan for assistance with surface analyses at the Center for Microanalysis of Materials, University of Illinois, which is supported by the Department of Energy under contract DE-AC 02-76ER 01198. K.S.S. gratefully acknowledges the receipt of an N.I.H. Research Career Development Award. The National Science Foundation supported this work.

References

1 **Suslick, K.S., ed.** *Ultrasound: Its Chemical, Physical, and Biological Effects* VCH Publishers, New York (1988)
2 **Apfel, R.E.** *Methods in Experimental Physics* Vol 19 (Ed. Edmonds, P.D.) Academic Press, New York (1981) 356–413
3 **Atcheley, A.A. and Crum, L.A.** *Ultrasound: Its Chemical, Physical and Biological Effects* (Ed., Suslick, K.S.) VCH Publishers, New York (1988)
4 **Neppiras, E.A.** *Phys Rep* (1980) **61** 159
5 **Suslick, K.S.** *Science* (1990) **247** 1373
6 **Suslick, K.S.** *Scient Am* (1989) **260** 80
7 **Margulis, M.A.** *Zh Fiz Khim* (1981) **55** 154
8 **Margulis, M.A.** *Zh Fiz Khim* (1985) **59** 1497
9 **Margulis, M.A.** *Ultrasonics* (1985) **23** 157
10 **Noltink, B.E. and Neppiras, E.A.** *Proc Phys Soc B* (1950) **63** 674; (1951) **64** 1032
11 **Hickling, R.** *J Acoust Soc Am* (1963) **35** 967
12 **Fogler, S.** *Can J Chem Eng* (1969) **47** 242
13 **Young, F.R.** *J Acoust Soc Am* (1976) **60** 100
14 **Fujikawa, S. and Akamatsu, T.** *J Fluid Mech* (1980) **97** 481
15 **Margulis, M.A. and Dmitrieva, A.F.** *Zh Fiz Khim* (1982) **56** 323
16 **Griffing, V.** *J Chem Phys* (1952) **20** 939
17 **Prudhomme, R.O. and Guilmart, T.** *J Chem Phys* (1957) **54** 336
18 **Golubnichii, P.I., Goncharov, V.D. and Proptopopov, Kh.V.** *Akusticheksii Zh* (1969) **15** 534
19 **Suslick, K.S., Gawienowski, J.W., Schubert, P.F. and Wang, H.H.** *J Phys Chem* (1983) **87** 2299
20 **Suslick, K.S., Gawienowski, J.J., Schubert, P.F. and Wang, H.H.** *Ultrasonics* (1984) **22** 425
21 **Suslick, K.S., Goodale, J.W., Schubert, P.F. and Wang, H.H.** *J Amer Chem Soc* (1983) **105** 5781
22 **Kruus, P. and Patraboy, T.J.** *J Phys Chem* (1985) **89** 3379
23 **Walton, A.J. and Reynolds, G.T.** *Adv Phys* (1984) **33** 595
24 **Jarman, P.D. and Taylor, K.J.** *Acustica* (1970) **23** 243
25 **Srinivasan, D. and Holroyd, L.V.** *J Appl Phys* (1961) **32** 446
26 **Jarman, P.D. and Taylor, K.J.** *Aust J Phys* (1970) **23** 319
27 **Sehgal, C., Sutherland, R.G. and Verrall, R.E.** *J Phys Chem* (1980) **84** 529
28 **Suslick, K.S. and Flint, E.B.** *Nature* (1987) **330** 553
29 **Flint, E.B. and Suslick, K.S.** *J Am Chem Soc* (1989) **111** 6987
30 **Sehgal, C.M. and Verrall, R.E.** *Ultrasound: Its Chemical, Physical and Biological Effects* (Ed., Suslick, K.S.) VCH Publishers, New York (1988)
31 **Gaydon, A.G.** *The Spectroscopy of Flames* Chapman and Hall, New York (1974)
32 **Wright, A.N. and Winkler, C.A.** *Active Nitrogen* Academic Press, New York (1968)
33 **Pearse, R.W.B. and Gaydon, A.G.** *The Identification of Molecular Spectra*, 4th edn, Wiley, New York (1976)
34 **Riesz, P., Berdahl, D. and Christman, C.L.** *Envr Health Per* (1985) **64** 233
35 **Henglein, A.Z.** *Naturforsch* (1985) **40b** 100
36 **Hart, E. and Henglein, A.** *J Phys Chem* (1986) **90**, 5992
37 **Tsang, W.** *Shock Waves in Chemistry* (Ed., Lifshitz, A.) Dekker, New York (1981) 59–130
38 **Suslick, K.S., Cline, Jr, R.E. and Hammerton, D.A.** *J Am Chem Soc* (1986) **108**, 5641
39 **Suslick, K.S., Cline, Jr, R.E. and Hammerton, D.A.** *IEEE Ultrason Symp Proc* (1985) **4** 1116
40 **Suslick, K.S. and Hammerton, D.A.** *IEEE Trans Ultrasonics Ferroelec Freq Contr* (1986) **33** 143
41 **Suslick, K.S. and Flint, E.B.** unpublished results
42 **Frenkel, Ya.I.** *Zh Fiz Khim* (1940) **14** 305
43 **Harvey, E.N.** *J Am Chem Soc* (1939) **61** 2392
44 **Degrois, M. and Baldo, P.** *Ultrasonics* (1974) **12** 25
45 **Kurochkin, A.K., Smorodov, E.A., Valitov, R.B. and Margulis, M.A.** *Zh Fiz Khim* (1986) **60** 646
46 **Kurochkin, A.K., Smorodov, E.A., Valitov, R.B. and Margulis, M.A.** *Zh Fiz Khim* (1986) **60** 1234
47 **Lauterborn, W. and Vogel, A.** *Ann Rev Fluid Mech* (1984) **16** 223

48 **Crum, L.A.** *Proc 1982 Ultrasonics Symp* (1982) **1** 1
49 **Preece, C.M. and Hansson, I.L.** *Adv Mech Phys Surf* (1981) **1** 199
50 **Doktycz, S.J. and Suslick, K.S.** *Science* (1990) **247** 1067
51 **Suslick, K.S.** *Modern Synthetic Methods* (1986) **4** 1
52 **Einhorn, C., Einhorn, J. and Luche, J.L.** *Synthesis* (1989) **11** 787
53 **Lindley, J. and Mason, T.J.** *Chem Soc Rev* (1987) **16** 275
54 **Suslick, K.S.** *Adv Organomet Chem* (1986) **25** 73
55 **Boudjouk, P.** *J Chem Ed* (1986) **63** 427
56 **Doktycz, S.J. and Suslick, K.S.** *Adv Sonochem* (1990) **1** in press
57 **Suslick, K.S. and Casadonte, D.J.** *J Am Chem Soc* (1987) **109** 3459
58 **Suslick, K.S., Casadonte, D.J. and Doktycz, S.J.** *Chem Materials* (1989) **1** 6
59 **Suslick, K.S. and Doktycz, S.J.** *J Am Chem Soc* (1989) **111** 2342
60 **Suslick, K.S., Casadonte, D.J. and Doktycz, S.J.** *Solid State Ionics* (1989) **43/33** 444
61 **Chatakondu, K., Green, M.L.H., Thompson, M.E. and Suslick, K.S.** *J Chem Soc Chem Commun* (1987) 900
62 **Suslick, K.S., Casadonte, D.J., Green, M.L.H. and Thompson, M.E.** *Ultrasonics* (1987) **25** 56
63 **Cole, R.H.** *Underwater Explosions* Princeton University Press, Princeton, NJ (1948)
64 **Vogel, A. and Lauterborn, W.** *J Acoust Soc Am* (1988) **84** 719